PROCEEDINGS, Thirty-Seventh Workshop on Geothermal Reservoir Engineering
Stanford University, Stanford, California, January 30 - February 1, 2012
SGP-TR-194

SUPERCRITICAL WATER JETS PENETRATING SUBCRITICAL WATER - APPLICATION FOR HYDROTHERMAL SPALLATION DRILLING

M. J. SCHULER, T. ROTHENFLUH, P. STATHOPOULOS, D. BRKIC, Ph. RUDOLF VON ROHR

ETH Zurich – Institute of Process Engineering
Sonneggstrasse 3
Zurich, CH-8092, Switzerland
e-mail: schulerm@ethz.ch

ABSTRACT

Spallation drilling is a promising alternative drilling technology that could prove to be economically advantageous over rotary techniques for drilling deep wells needed e.g. for geothermal energy production. This drilling technique uses the properties of certain rock types to disintegrate into small disk-like fragments due to thermal stresses when heated up rapidly by a highly energetic jet.

In water (resp. water based drilling fluid) filled boreholes at depths below 2 kilometers water exceeds its critical pressure (220.64bar) and hydrothermal flames can be applied to provide the required heat to spall the rock. One such potential spallation drilling head consists of a combustion chamber fed by water, fuel and an oxidant. Fuel and oxidant are preheated and form a supercritical (> 220.64bar, >373.95°C) hydrothermal flame in the aqueous environment of the burning chamber. The water present in the combustion chamber is thus heated up to high, supercritical temperatures and ejected through a nozzle together with the combustion products. This highly energetic supercritical water jet is directed towards the rock surface to induce fragmentation.

Thus a hot supercritical water jet is operated downhole in a dense, aqueous environment (drilling fluid) at mostly subcritical conditions. With such a setup, high heat transfer rates from the supercritical water jet towards the cold and dense environment (drilling fluid) are detected as major drawback. The significant velocity, density and enthalpy differences in between the hot jet and the environment result in huge entrainment rates of cold fluid and finally in a rapid temperature decay in the jet. This entrainment effect decreases the overall efficiency of the hydrothermal spallation drilling process significantly.

Experiments are conducted in a high pressure reactor with optical access equipped with a preheating and injection system providing submerged supercritical water jets for varying nozzle exit temperatures, mass flow rates and nozzle diameters in order to investigate pseudo critical penetration length (≥375.21°C at 224bar), shape and overall heat transfer for a wide range of operating conditions. In the experiments two different methods were applied and compared with each other. The pseudo critical penetration length was investigated by axial temperature measurements with a mantel thermocouple and a novel optical Schlieren method based on the strong change of the refractive index around the pseudo critical point of water. A good agreement in between both methods was determined.

Additionally a numerical model based on the commercial CFD tool (ANSYS FLUENT® 12.1) was developed to gain deeper inside into the behavior of such jets. Conservation of momentum, mass and energy including the thermo physical properties of water were the basis of the model. In case of a round jet at high Reynolds numbers, the realizable k-ε turbulence model was used. Finally all numerical results were validated with the experimental measurements and show an acceptable agreement.

The major finding of this investigation was the fact, that for almost all operating conditions applied in the experiments, the supercritical penetration length of the jet was always roughly in the range of the nozzle diameter. Thus increasing the jet's nozzle exit temperature or the mass flow rate of supercritical water does not elongate the jet due to enhanced entrainment and turbulent mixing with cold subcritical environment. The developed model was able to predict the experimentally detected trends and show an acceptable agreement with measurements.

1. INTRODUCTION - BACKGROUND AND MOTIVATION

The "spallation drilling" (**SD**) technology is known as a promising alternative drilling technology that could prove to be economically advantageous over rotary techniques for drilling deep wells in hard rock formations. Enhanced drilling velocities and less frequent replacement of the drilling head are expected as major advantages. Hence it is assumed that drilling costs could be significantly reduced [1]. Several promising scientific investigations and field tests applying SD at ambient conditions for drilling shallow holes are available in literature [2-6]. But for drilling wells of several kilometers depth, a (water based) drilling fluid is essentially required to fulfill several important tasks in the drilling process, e.g. removal of rock cuttings. In deep heat mining projects for the production of electricity out of geothermal energy, such deep holes are required [7]. A e.g. water based drilling fluid has to be present in borehole and hence SD in such a environment is named "hydrothermal spallation drilling" (**HSD**) [8]. In the HSD process, a hot fluid jet or a flame jet in an aqueous environment impinges on the upper rock layer at the bottom of the borehole. Due to the low thermal conductivity of rock, only the upper rock layer is heated up rapidly and steep temperature gradients are induced. Thermal expansion of this hot layer cause high thermal stress till this upper layer fracture into small fragments [3, 6, 9]. During HSD, this mechanism is repeated again and again and finally results in the drilling progress.

In a water (resp. water based drilling fluid) filled borehole at depths below 2 kilometers, water exceeds its critical pressure (220.64bar) and thus hydrothermal flames are favored to provide the required heat to spall the rock formation. Such flames are used in the supercritical water (>220.64bar, >373.95°C) oxidation (**SCWO**) process to combust and thus destroys hazardous organic components [10-12]. One such potential spallation drilling head consists of a combustion chamber fed by water, fuel and an oxidant. Fuel and oxidant are preheated and form a hydrothermal flame in the aqueous environment of the combustion chamber. The water present in the chamber is thus heated up to high, supercritical temperatures and ejected through a nozzle together with the combustion products [13]. The highly energetic mostly supercritical water jet is finally directed towards the rock surface to induce thermal fragmentation. Thus a submerged supercritical water jet can be seen as a possible downhole approach for the HSD technology [13, 14]. Several challenges have to be tackled in order to transfer the ambient SD technology into the aqueous and dense environment of HSD. For example downhole ignition and stable operation of a hydrothermal flame is still a challenging task. Transport of rock cuttings and decay of drilling fluid additives due to the required heat is also an unsolved problem. The heat transfer of the impinging hot jet towards the rock surface is one of the crucial parameters in HSD. Heat losses from the hot jet towards the cold environment by means of entrainment are additional challenges in comparison to SD at low dense ambient conditions [13].

Only two investigations of submerged supercritical water jets are available in literature. Experiments by Augustine et al. [8] concentrate on the thermal far field of this kind of jets. The hot super respectively pseudo critical plume (see Figure 3) in the developing zone of the jet is of major interest for HSD because temperatures above 350°C are required to reach onset of spallation [3, 4, 15]. Heat losses in this region are crucial for the efficiency of the overall process because heat is transferred to the cold environment instead to the rock surface. Therefore this region was investigated experimentally by Rothenfluh et al. [14] in our research group.

The possibility to apply submerged supercritical water jets within this economically interesting HSD technology is also the motivation behind the presented investigation. In the experiments supercritical water (**SCW**) surrounded by a slowing co-flowing cooling water (**CW**) stream (20°C) was injected through the injection system in gravitational direction into a high pressure vessel (see also Figure 3). The used experimental setup is part of a test facility originally used in SCWO processes [16]. In Figure 1, the experimental setup including all needed devices in the experiments is illustrated. Optical access to the high pressure vessel is given by 4 sapphire glass windows within two planes.

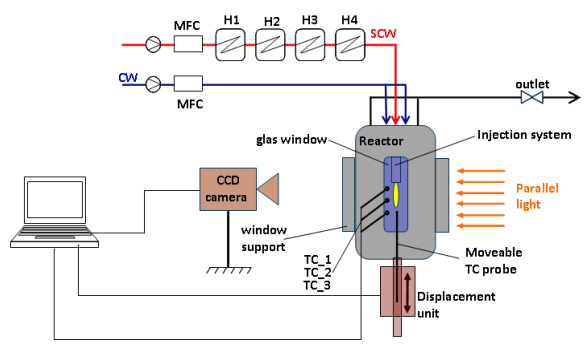

Figure 1: Used high pressure setup in the supercritical water jet study.

A high precision linear displacement unit was mounted at the bottom of the reactor to enable axial temperature measurements. Several K-type thermocouples (**TC**) were installed in the reactor to control and record the temperature distribution inside the reactor. Four electrical heating units (**H1-H4**) were installed for heating up the water stream to supercritical conditions before entering the reactor.

The mass flow rates of CW and SCW were controlled by mass flow controllers (**MFC**). Besides the injection system, the outlets of the reactor are located on top of the reactor. For the optical measurements [14], parallel light rays were incorporated into the reactor and detected after passing through the supercritical water jet by the installed CCD camera. Submerged supercritical water jets for varying nozzle exit temperatures T_0, mass flow rates and nozzle diameters were investigated. Pseudo critical penetration length (**PCPL**), shape and overall heat transfer were detected for a wide range of operating conditions. The distance from nozzle outlet to the position of the pseudo critical temperature (**PCT**) of water (224bar, 375.21°C) on the jet axis was defined as PCPL (see Figure 3). A detailed description of the whole experimental setup and the applied methods can be found in reference [14].

In the experiments two different methods were applied and compared with each other and finally showed a good agreement. The submerged supercritical water jet was investigated by axial temperature measurements with a K-type mantel thermocouple (Ø 0.25mm, class 1) and a novel optical Schlieren method based on the strong change of the refractive index around the pseudo critical point (**PCP**) [14]. For an operating pressure of 224bar in the reactor, the pseudo critical temperature of water is 375.21°C. All thermo physical properties undergo strong changes in the vicinity of the PCP [17-19]. Especially the heat capacity at constant pressure (cp) reaches high values in the appearing peak. In Figure 2, the dimensionless change of the thermo physical properties of water at 224bar with respect to temperature is illustrated. All plotted properties are normalized with the value at 25°C and 224bar.

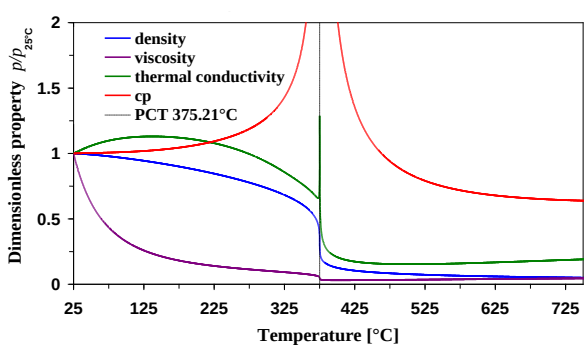

Figure 2: Normalized thermo physical properties of water at 224bar as a function of temperature (normalized with the value at 25°C and 224bar) [17-19].

An experimental image of a submerged supercritical water jet leaving the nozzle is shown in Figure 3 including all relevant parameters and definitions [14]. The pseudo critical temperature isotherm (375.21°C) was detectable in the time averaged images by an enveloping line of minimum gray values around the pseudo critical plume. The tip of this line was defined as PCPL. The maximal change of the reflective index occurs at the PCP of water and this finally results in the minimum gray values of the images.

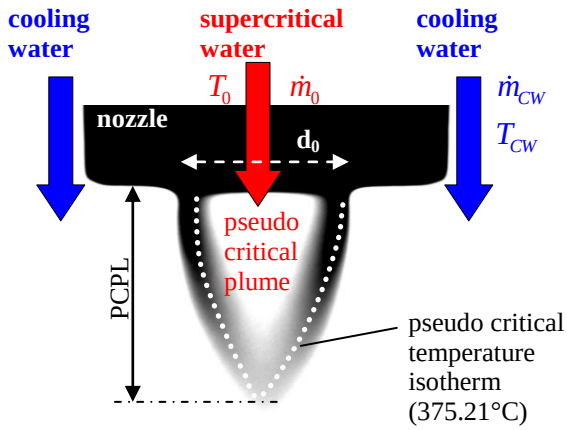

Figure 3: Experimental picture of a supercritical water jet (224bar) for a nozzle diameter of d_0=3mm including all relevant parameters, variables and definitions.

$\dot{m}_0 = mass\ flow rate\ SCW$

$T_0 = nozzle\ exit\ temperature\ SCW$

$d_0 = nozzle\ diameter$

$\dot{m}_{CW} = mass\ flow rate\ CW$

$T_{CW} = exit\ temperature\ CW$

A experimental setup for the investigation of water in its supercritical state has only limited experimental access due to the challenging temperature and pressure conditions [16]. Also the applied methods and measurement devices have to withstand and work at high temperatures and pressures in an aqueous environment [14]. Hence in case of such harsh conditions, CFD (Computational Fluid Dynamics) methods are widely-used as powerful tool for gaining deeper inside into the systems that could not be realized by means of experimental measurements [11, 12, 20, 21].

Hence a theoretical model based on the commercial CFD tool ANSYS FLUENT® (12.1) was developed to investigate heat transfer phenomena of submerge supercritical water jets [22, 23]. The conservation equations of momentum, mass and energy were the basis of the model. In case of a round jet at high Reynolds numbers, the realizable k-ε turbulence model [24] is suggested. All thermo physical properties of water were implemented in the model based on the REFPROP® 8.0 database [17]. Finally, all theoretical results based on the model were validated with experimental measurements by Rothenfluh et al. [14].

2. DEVELOPMENT OF THE NUMERICAL MODEL

2.1 Governing equations and turbulence

The conservation equations for momentum and mass were solved as Favre-averaged Navier-Stokes equations. In order to close these equations, the Reynolds stresses had to be modeled properly. This task was fulfilled by a two equation turbulence model out of the k-ε family and the introduction of the eddy viscosity and Boussinesq approach [23, 25, 26]. In case of a round jet at high Reynolds numbers, the realizable k-ε model [24] is recommended. Finally the energy conservation equation was included in the model to describe a non-isothermal jet [22, 23].

2.2 Geometry and computational domain

In the spallation drilling process, rock surface temperatures around 500°C [4, 15] are suggested. Thus the supercritical jet region is of major interest regarding HSD. The fully developed region of the jet further downstream from the nozzle was less relevant for this investigation. Therefore only the inner axisymmetric part of the reactor including coaxial injector system was simulated as a confined setup along the axis of symmetry considering 2D axisymmetric coordinates. (radius 18.2mm, length 123.5mm). All solid parts of the injection system were constructed out of steel INOX V4A (316L). An air gap insulation in between inner hot stream and cold annular water flow was realized within the injector in order to minimize heat losses. Injectors with nozzle diameters of 1mm, 2mm, 3mm and 4mm were used. The grid generator GAMBIT® (2.2.30) was used to mesh the computational domain. In all simulations, structured grids with a total number of cells in between 800`000 to 2`000`000 were required to guarantee a mesh independent solution. Enhanced wall treatment was applied in the whole domain. Mass-flow-inlet boundary conditions for all incoming streams into the reactor were used. Pressure outlet boundary conditions were chosen as boundary condition for the effluent flows [22, 23].

2.3 Thermo physical properties of water

All required thermo physical properties of water were implemented into the numerical model over the whole rage of experimental conditions. For the simulation of compressible water flow with single phase CFD methods, five different fluid properties are needed (density ρ, heat capacity at constant pressure cp, thermal conductivity λ, dynamic viscosity μ and speed of sound a) [22]. The available routines of REFPROP® 8.0 [17-19] were used in all calculations of thermo physical properties. Uncertainties of the used data base can be found in literature [17]. All properties were implemented in the commercial CFD-code ANSYS FLUENT® via user defined functions (UDF) at predefined interfaces [27]. Constant material properties in the solid steel parts (316L) were assumed according to the data sheet of the supplier. Properties of air in the gape insulation were calculated for ambient conditions [17].

2.4 Solution procedure

The ANSYS FLUENT® pressure based coupled solver was applied considering 2D axisymmetric coordinates. Steady state simulations excluding gravitation and viscous heating were performed. Second-order scheme for pressure and second order upwind schemes for all other variables were chosen for spatial discretization. Gradients were evaluated by the Least-Squares-Cell-Based method [22, 23]. Default values in ANSYS FLUENT® were used for all model constants. Only the turbulent energy Prandtl number was reduced from 0.85 to 0.7 as recommended in literature for turbulent round jets [28]. In the simulations, the residual values for each variable have to fall at least three orders of magnitude (energy below 10^{-6}).

3. RESULTS AND DISCUSSION

3.1 Pseudo critical penetration length (PCPL)

Within this paragraph a few theoretical results of the computational model were compared with optically detected experimental values of the PCPL by Rothenfluh et al. [14]. In this submerged supercritical water jet study, two different series were performed. In the first serial, mass flow rates of co-flowing cooling water (65 g/s) and supercritical water (4 g/s) were kept constant. The exit temperature of cooling water T_{CW} was always 20°C. The influence of varying nozzle exit temperatures T_0 regarding the pseudo critical penetration length was investigated. In Figure 4, a comparison in between experimental and numerical results for a nozzle diameter of 3mm is shown. In Figure 4 (a), the experimental data proof that with increasing nozzle exit temperatures, the PCPL is decreasing. For temperatures near the PCP, the decrease is significant. Towards higher temperatures, only a slight decrease of the PCPL is recorded. There is an acceptable agreement in between experiment and simulation. The calculated PCPL follows the experimental trend of decreasing length with increasing nozzle exit temperatures till a local minimum in the PCPL at 425°C. Afterwards for increasing temperatures, a slight increase in the simulated PCPL occurs.

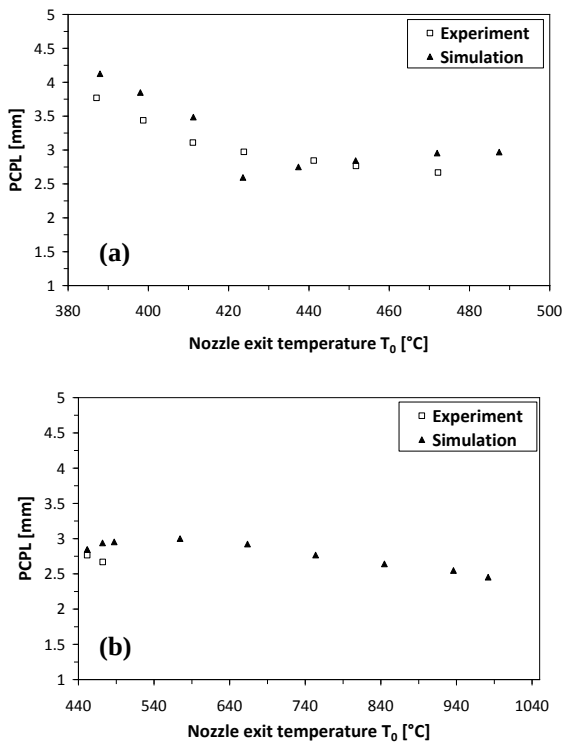

Figure 4: Comparison in between optically detected pseudo critical penetration length (PCPL) and numerical results with the applied realizable k-ε model for a nozzle diameter of 3mm and varying jet nozzle exit temperatures T_0 at constant SCW mass flow rate (4 g/s); CW mass flow rate (65 g/s) and the CW temperature (20°C) were kept constant.

When the developed model was used as a prediction tool, the possibility to investigate nozzle exit temperatures out of the experimental range was given. Results of this approach are shown in Figure 4 (b). The slight increase in the calculated PCPL propagates till a nozzle outlet temperature of roughly 575°C. Afterwards a slight decrease is detected.

The observed general trend in Figure 4 is explainable with the change of the thermo physical properties of water with respect to temperature. The significant decrease of the PCPL after the PCP is directly linked to the strongly varying properties in this region. Around the PCP, the pseudo phase change (**PPC**) of water occurs and thus water in a liquid like state passes over towards a dense gas state (or vice versa). Thus the material properties also change to a more gas like behavior and therefore a gas like jet was operated in a liquid like environment. For temperature variations above the PPC, the thermo physical properties of water depend almost linear on temperature (see also Figure 2). Due to the huge density, enthalpy and velocity differences in between SCW jet and surrounding cooling water, significant entrainment rates of cold ambient water occurred. By increasing the nozzle exit temperature T_0 at a constant SCW mass flow rate, velocity, enthalpy and density differences were also raising. This fact finally favors entrainment and turbulent mixing and thus decreases the PCPL.

In a second serial, mass flow rate of co-flowing cooling water (65g/s) and CW exit temperature (20°C) were kept constant. Also the nozzle exit temperature T_0 (410°C) was fixed. Only the mass flow rate of SCW was varied within the experiments and simulations. Results of this serial are plotted in Figure 5.

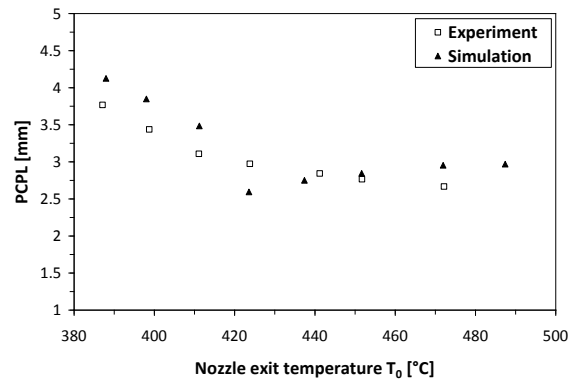

Figure 5: Comparison of the optically detected PCPL with simulated values for varying SCW mass flow rates; nozzle exit temperature T_0 (410°C), T_{CW} (20°C) and cooling water mass flow rate (65g/s) were kept constant for a nozzle diameter of 3mm with the applied realizable k-ε turbulence model.

Also for this second serial, an acceptable agreement between experiment and simulation was shown. With increasing mass flow rates of SCW, the PCPL nearly stays unchanged in the experiment as well as in the simulation. The recorded values of the PCPL in the investigated range were all around the nozzle diameter (3mm). In comparison to experimental data, simulated values were slightly over predicted for increasing SCW mass flow rates. For higher mass flow rates at constant T_0, more energy was provided by the SCW jet: The density and enthalpy difference between jet and cooling water was always the same in this second serial. The nozzle exit velocity was increasing with the SCW mass flow rate. The additional energy input was not able to elongate the pseudo critical plume, because higher velocity differences favor entrainment and turbulent mixing. These effects compensate the additional energy input and finally result in a nearly constant PCPL.

3.2 Space and time averaged overall heat transfer coefficient

In the direct contact steam condensation (**DCSC**) process, superheated steam is injected into a cold

stagnant water bath to study the heat transfer during the condensation process. By means of experimental data in the two phase region of water, the time and space averaged overall heat transfer coefficient can be calculated based on an energy balance and the assumption that the limiting step is the condensation process [29-35].

In case of a supercritical water jet operated in a subcritical water environment, this approach could also be applied to get an idea of the heat transfer coefficient. The overall heat transfer coefficient (k) was calculated with an energy balance. The made assumption was that the energy injected by the SCW jet $\dot{m}_0 \cdot (h_0 - h_{PCT})$ has to be transferred through the smooth isothermal surface area (A_{PCT}) at the PCP to the subcritical cooling water environment that further pseudo phase change can occur (see also Figure 2 and 3). The driving temperature difference $(T_{PCP} - T_{CW})$ for the heat transfer was estimated by the difference in between the temperature at the PCP of water (375.21°C) and the cooling water (20°C). Hence the overall heat transfer coefficient could be estimated according to equation 1.

$$k = \frac{\dot{m}_0 \cdot (h_0 - h_{PCT})}{A_{PCT} \cdot (T_{PCP} - T_{CW})} \qquad (1)$$

A smooth surface area of parabolic shape was assumed in the calculation step of A_{PCT}. Hence PCPL and nozzle diameter were required to calculate the surface area A_{PCT} where the pseudo phase change of water occurred. The specific enthalpy values for the nozzle exit condition (h_0) and the PCT (h_{PCT}) were based on the REFPROP 8.0 database [17]. The approach explained above was applied to the experimental data of the supercritical water jet study and finally results in Figure 6. In there, the space and time averaged overall heat transfer coefficient is plotted as a function of the dimensionless penetration length (PCPL/d_0) for different nozzle diameters.

In comparison to direct contact steam condensation, higher values for the overall heat transfer coefficient were evaluated for SCW jets [29, 36]. This is due to the fact, that the limiting step of condensation and latent heat removal in the boundary layer did not take place above the two phase region of water. In case of a submerged SCW jet, the heat transfer is primarily controlled by turbulent mixing. An increasing heat transfer coefficient was detected for decreasing nozzle diameters and increasing SCW mass flux. This findings are consistent with the DCSC process [29].

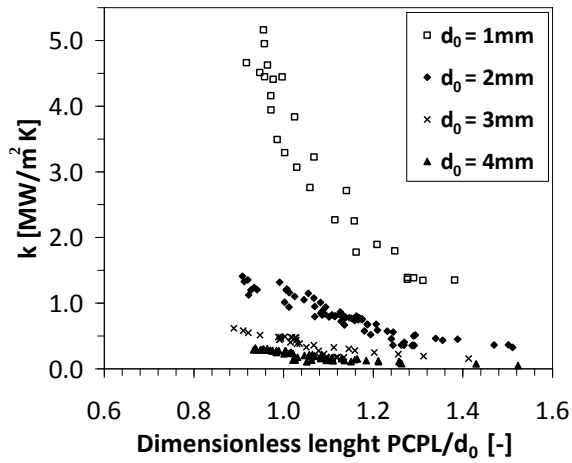

Figure 6: Time and space averaged overall heat transfer coefficient for submerged supercritical water jets in a subcritical cooling water environment as a function of the dimensionless penetration length over a wide range of experimental conditions [14] and for different nozzle diameters.

Figure 6 also proofs the decreasing PCPL with increasing T_0 and nearly independent values of the PCPL for increasing SCW mass flow rates as mentioned above. The shortest dimensionless lengths (PCPL/d_0) were determined for the highest differences (density, velocity and enthalpy) in between SCW and CW flow. For high values of T_0 in the first serial and high SCW mass flow rates in the second serial, such conditions were applied. Under these settings, the highest overall heat transfer coefficients were evaluated.

4. CONCLUSION

Submerged supercritical water jets were studied experimentally for a wider rage of experimental condition. The pseudo critical penetration length was investigated at a set operating pressure of 224bar for varying nozzle exit temperature and supercritical mass flow rates. At this pressure level, critical and pseudo critical temperature of water are close together. For almost all operating conditions applied in the experiments, the pseudo critical penetration length of the jet was always roughly in the range of the nozzle diameter. Only for nozzle exit temperatures near the pseudo critical point, elevated values for the PCPL were detected. Increasing the jet's nozzle exit temperature or the mass flow rate of supercritical water does not elongate the jet. Hence the additional energy input is compensated due to enhanced entrainment and turbulent mixing with the cold subcritical environment.

Additionally a numerical model based on commercial CFD tool ANSYS FLUENT® was developed and

applied to submerged supercritical water jets. In the validation step with experimental data of Rothenfluh et al., acceptable agreement between experiment and simulation was achieved. The trends detected in the experiments were predicted reasonably well by the model.

The heat transfer mechanisms of the DCSC process in the two phase region of water were finally compared with submerged supercritical water jets. In contrast to DCSC, the PCPL of SCW jets could not be elongated by increasing the jet's nozzle exit temperature or the SCW mass flow rate, because the additional energy input at the nozzle is directly lost to the subcritical water environment due to enhanced entrainment and turbulent mixing effects. The latent heat release during condensation in the DCSC process has to be transported away to the liquid bath. According to literature, this step is detected as limiting mechanism leading to penetration lengths much longer than those found for submerged SCW jets. Such a limiter was not determined for the pseudo phase change of water and thus higher values for the heat transfer coefficients were evaluated dominated by turbulent mixing effects.

REFERENCES

1. Potter, R.M. and J.W. Tester, Drilling of Vertical Boreholes by Thermal Processes: Including Rock Spallation and Fusion, U.S. Patent No. 5'771'984. 1998.
2. Browning, J.A., W.B. Horton, and H.L. Hartman. Recent Advances in Flame-jet Working of Minerals. in 7th Symposium on Rock Mechanics. 1965. Pennsylvania State University: Society of Mining Engineers.
3. Rauenzahn, R.M. and J.W. Tester, Rock Failure Mechanisms of Flame-Jet Thermal Spallation Drilling - Theory and Experimental Testing. International Journal of Rock Mechanics and Mining Sciences & Geomechanics Abstracts, 1989. 26(5): p. 381-399.
4. Williams, R.E., R.M. Potter, and S. Miska, Experiments in thermal spallation of various rocks. Journal of Energy Resources Technology-Transactions of the Asme, 1996. 118(1): p. 2-8.
5. Poirier, S., et al., Thermal rock fragmentation - Applications in narrow-vein extraction. Cim Bulletin, 2003. 96(1071): p. 66-71.
6. Preston, F.W. and H.E. White, Observations on spalling. Journal of the American Ceramic Society, 1934. 17: p. 137-144.
7. The Future of Geothermal Energy, MIT press , Cambridge (2006), http://geothermal.inel.gov/publications/future_of_geothermal_energy.pdf.
8. Augustine, C.R., Hydrothermal spallation drilling and advanced energy conversion technologies for engineered geothermal systems. PhD thesis, Massachusetts Institute of Technology, 2009.
9. Williams, R.E., The Thermal Spallation Drilling Process. Geothermics, 1986. 15(1): p. 17-22.
10. Von Rohr, P.R., K. Prikopsky, and T. Rothenfluh, Flames in supercritical water and their applications. Strojnicky Casopis, 2008. 59(2): p. 91-103103.
11. Bermejo, M.D. and M.J. Cocero, Supercritical water oxidation: A technical review. AIChE Journal, 2006. 52(11): p. 3933-3951.
12. Augustine, C. and J.W. Tester, Hydrothermal flames: From phenomenological experimental demonstrations to quantitative understanding. Journal of Supercritical Fluids, 2009. 47(3): p. 415-430.
13. Rothenfluh, T., P. Rudolf Von Rohr, and M. Schuler, Method of thermal rock fragmentation in borehole involves feeding reactants to downhole assembly in borehole, and performing exothermic reaction of reactants in reaction zone in presence of water-based drilling fluid, ETH ZUERICH (ETHZ-Non-standard). p. 63.
14. Rothenfluh, T., M.J. Schuler, and P.R. von Rohr, Penetration length studies of supercritical water jets submerged in a subcritical water environment using a novel optical Schlieren method. The Journal of Supercritical Fluids. 57(2): p. 175-182.
15. Wilkinson, M.A. and J.W. Tester, Experimental-Measurement of Surface Temperatures During Flame-Jet Induced Thermal Spallation. Rock Mechanics and Rock Engineering, 1993. 26(1): p. 29-62.
16. PRIKOPSKY, K., Characterization of continuous diffusion flames in supercritical water, in Institute of Process Engineering. 2007, no. 17'374, ETH Zurich, (http://www.e-collection.ethz.ch): Zurich, Switzerland.
17. Lemmon, E.W., M.L. Huber, and M.O. McLinden, NIST Standard Reference Database 23: Reference Fluid Thermodynamic and Transport Properties-REFPROP, Version 8.0. 2007, National Institute of Standards and Technology: Gaithersburg. p. Standard Reference Data Program.
18. Wagner, W. and A. Pruss, The IAPWS formulation 1995 for the thermodynamic properties of ordinary water substance for general and scientific use. Journal of Physical

and Chemical Reference Data, 2002. 31(2): p. 387-535.

19. Kestin, J., et al., THERMO-PHYSICAL PROPERTIES OF FLUID H2O. Journal of Physical and Chemical Reference Data, 1984. 13(1): p. 175-183.
20. Lieball, K., Numerical Investigations on a transpiring wall reactor for supercritical water oxidation, in Institute of Process Engineering. 2003, no. 14'911, ETH Zurich, (http://www.e-collection.ethz.ch): Zurich, Switzerland.
21. Narayanan, C., et al., Numerical modelling of a supercritical water oxidation reactor containing a hydrothermal flame. Journal of Supercritical Fluids, 2008. 46(2): p. 149-155.
22. ANSYS FLUENT User`s Guide. 2010, ANSYS Inc.
23. ANSYS FLUENT Theory Guide. 2010, ANSYS Inc.
24. Shih, T.H., et al., A NEW KAPPA-EPSILON EDDY VISCOSITY MODEL FOR HIGH REYNOLDS-NUMBER TURBULENT FLOWS. Computers & Fluids, 1995. 24(3): p. 227-238.
25. Pope, S.B., Turbulent Flows. 2000, Cornell: Cambridge University Press.
26. Versteeg, H.K. and W. Malalasekera, An Introduction to Computational Fluid Dynamics. Second Edition ed. 2007, Edinburgh: Pearson Education Limited.
27. ANSYS FLUENT UDF MANUAL. 2010, ANSYS Inc.
28. Brinckman, K.W., W.H. Calhoon, and S.M. Dash, Scalar fluctuation modeling for high-speed aeropropulsive flows. Aiaa Journal, 2007. 45(5): p. 1036-1046.
29. Kim, H.Y., et al., Experimental study on stable steam condensation in a quenching tank. International Journal of Energy Research, 2001. 25(3): p. 239-252.
30. Kim, Y.S., J.W. Park, and C.H. Song, Investigation of the steam-water direct contact condensation heat transfer coefficients using interfacial transport models. International Communications in Heat and Mass Transfer, 2004. 31(3): p. 397-408.
31. Aya, I. and H. Nariai, EVALUATION OF HEAT-TRANSFER COEFFICIENT AT DIRECT-CONTACT CONDENSATION OF COLD WATER AND STEAM. Nuclear Engineering and Design, 1991. 131(1): p. 17-24.
32. Gulawani, S.S., et al., CFD simulation of flow pattern and plume dimensions in submerged condensation and reactive gas jets into a liquid bath. Chemical Engineering Science, 2008. 63(9): p. 2420-2435.
33. Gulawani, S.S., et al., Analysis of flow pattern and heat transfer in direct contact condensation. Chemical Engineering Science, 2009. 64(8): p. 1719-1738.
34. Gulawani, S.S., et al., Submerged gas jet into a liquid bath: A review. Industrial & Engineering Chemistry Research, 2007. 46(10): p. 3188-3218.
35. Gulawani, S.S., et al., CFD analysis of flow pattern and heat transfer in direct contact steam condensation. Chemical Engineering Science, 2006. 61(16): p. 5204-5220.
36. Chun, M.H., Y.S. Kim, and J.W. Park, An investigation of direct condensation of steam jet in subcooled water. International Communications in Heat and Mass Transfer, 1996. 23(7): p. 947-958.